JFE TECHNICAL REPORT
No. 24 (Mar. 2019)

Development of Welding Technologies for Automotive Chassis

KITANI Yasushi[*1] MATSUDA Hiroshi[*2] MATSUSHITA Muneo[*3] YAMAMOTO Shunsuke[*4] ANDO Satoru[*5]
IKEDA Rinsei[*6]

1. Introduction

Automotive chassis (undercarriage) parts are no exception to the need for auto body weight reduction to improve fuel economy. In response to this need, high strength high tensile steel materials have also been applied to chassis parts in recent years, and their usage ratio has tended to increase. Rigidity and durability are particularly important because the chassis plays the role of supporting the weight of the auto body and absorbing cyclical load changes during travel, and for this reason, hot-rolled steel sheets with larger thicknesses than those of body parts are frequently used. Gas shielded arc welding in the form of lap fillet joints is mainly used in manufacturing chassis parts, and fatigue strength is the most important property requirement for welded joints. It is known that the fatigue strength of welded joints cannot be increased by using higher strength steel sheets because the fatigue properties of joints are governed by stress concentration on the weld bead. Therefore, improving the fatigue strength of welded joints is the most critical issue for welding chassis parts when using high tensile steel materials.

Moreover, corrosion resistance (rust resistance) is also important from the viewpoint of durability because chassis parts are exposed to an environment where rust easily occurs due to water is splashed from the road surface during travel. Although chassis parts are painted to guarantee corrosion resistance, the fact that the paintability of gas shielded arc welds is reduced by slag adhering to the weld bead surface, and as a result, the corrosion resistance of the chassis parts is reduced, is viewed as a problem.

As outlined above, improvement of the fatigue strength and corrosion resistance of welded joints is strongly desired in welding technologies applied to the automotive chassis. If the fatigue strength and corrosion resistance of the joints are not improved, the merit of reduction of sheet thickness by using high-tensile steel materials cannot be obtained, and it will also be difficult to realize weight reduction of the parts. As welding technologies which make it possible to improve the fatigue strength and corrosion resistance of welded joints in comparison with conventional gas shielded arc welding, this paper introduces a low CO_2 gas shield arc

† Originally published in *JFE GIHO* No. 41 (Feb. 2018), p. 55−61

*1 Dr. Eng.,
Senior Researcher Deputy General Manager,
Joining & Strength Research Dept.,
Steel Res. Lab.,
JFE Steel

*2 Dr. Eng.,
Senior Researcher General Manager,
Joining & Strength Research Dept.,
Steel Res. Lab.,
JFE Steel

*3 Ph. D.,
Senior Researcher Deputy General Manager,
Joining & Strength Research Dept.,
Steel Res. Lab.,
JFE Steel

*4 Senior Researcher Deputy Manager,
Coated Products Research Dept.,
Steel Res. Lab.,
JFE Steel

*5 Dr. Eng.,
Senior Researcher Deputy General Manager,
Coated Products Research Dept.,
Steel Res. Lab.,
JFE Steel

*6 Dr. Eng.,
General Manager,
Joining & Weldability Evaluation Center,
Structural Materials Solution Div.,
JFE Techno-Research

Copyright © 2019 JFE Steel Corporation. All Rights Reserved.

welding technology using a shielding gas with a low CO_2 composition and a Plasma-Arc Hybrid™ welding technology. In addition, this paper also touches on the development of a laser-arc hybrid welding technology as a high efficiency, high quality welding technology responding to changes in the structure of chassis parts.

2. Low CO_2 Gas Shielded Arc Welding Technology

2.1 Problems to be Solved by Low CO_2 Gas Shielded Arc Welding

There is a large need for improvement of the fatigue strength and corrosion resistance of joints in gas shielded arc welding of chassis parts. Because stress concentration at the weld toe is the dominant factor for the fatigue characteristics of welded joints, it is difficult to obtain a joint fatigue strength improvement effect by adopting high-tensile strength steels. Moreover, since corrosion reduces the thickness of steel sheets regardless of the strength of the steel sheet, an increase in steel strength cannot contribute to a decrease in the sheet thickness. Slag adhering to the weld bead and/or weld toe causes paint film defects. Corrosion starts from those defects and proceeds into the steel. Although the fatigue strength of joints is reduced by stress concentration at the weld toe, a further decrease in fatigue strength by reduction of the sheet thickness by corrosion is also a concern in the use environments of actual vehicle. To solve these problems, JFE Steel studied and developed the application of a low CO_2 gas shielded arc welding method, which is a gas shielded arc welding method with a reduced mixing ratio of the active gas (CO_2). As a result, the toe shape of the toe bead was improved and corrosion resistance of the toe bead was enhanced, and an arc welding technology which enables a large improvement in the fatigue characteristics of chassis parts in actual use was developed[1–3].

2.2 Change of Weld Bead Shape by Shielding Gas Composition[1)]

Photo 1 shows the cross-sectional macrostructures of lap fillet joints (sheet thickness: 2.3 mm, 400 MPa grade hot-rolled steel sheet). Ar-20% CO_2 and Ar-5% CO_2 mixed gases are used for the shielding gas, which are in conventional MAG and reduced CO_2 conditions, respectively. It can be understood that the weld toe shape is flattened by reduction of the CO_2 in the shielding gas. **Figure 1** shows the results of measurements of the weld surface profile with a laser displacement meter and the results of calculations of the stress distribution during plane bending loading by FEM. The FEM analysis was conducted using a model with the shape obtained from the measurement results. (The steel, including the weld, was assumed to be completely homogeneous; Young's modulus of 206 000 N/mm^2, a Poisson ratio of 0.3 and density of 7.85 g/m^3 were given.) The stress distribution in the figure is under loading of 247N. Although a stress concentration occurred around the weld toe, the toe was flattened by reducing the CO_2 mixing ratio from 20% to 5%, and the maximum tensile stress acting on the toe decreased by 11%.

2.3 Influence of Shielding Gas Composition on Corrosion Behavior of Arc Welds[2)]

A corrosion test was performed (repetition of cycle of salt water immersion → drying → humidity) for the

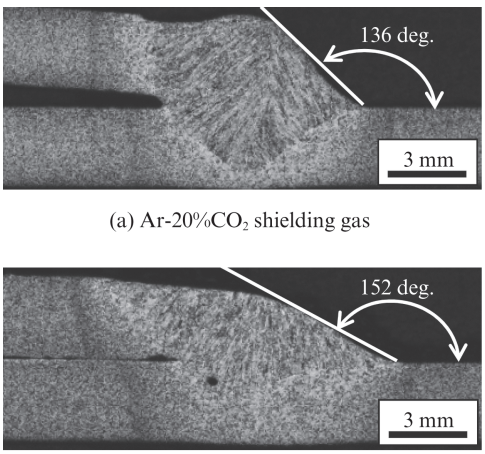

(a) Ar-20%CO_2 shielding gas

(b) Ar-5%CO_2 shielding gas

Photo 1 Cross-sectional macrostructures of lap-fillet welds

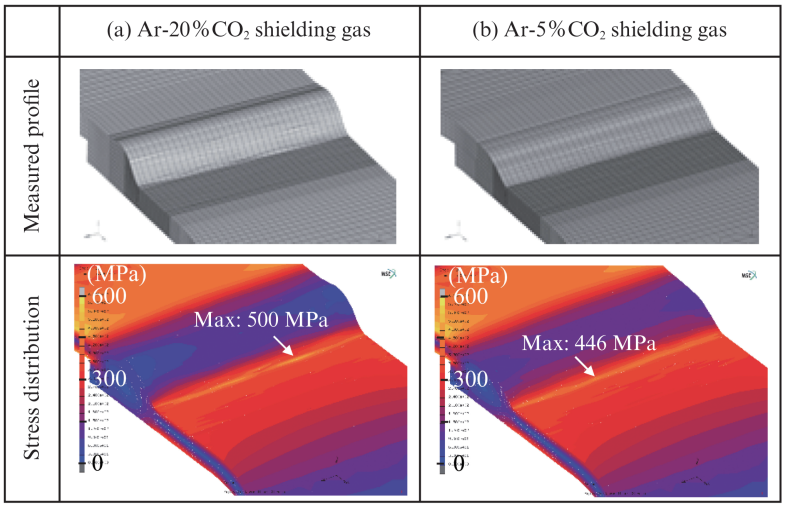

Fig. 1 Calculated stress distributions around weld part

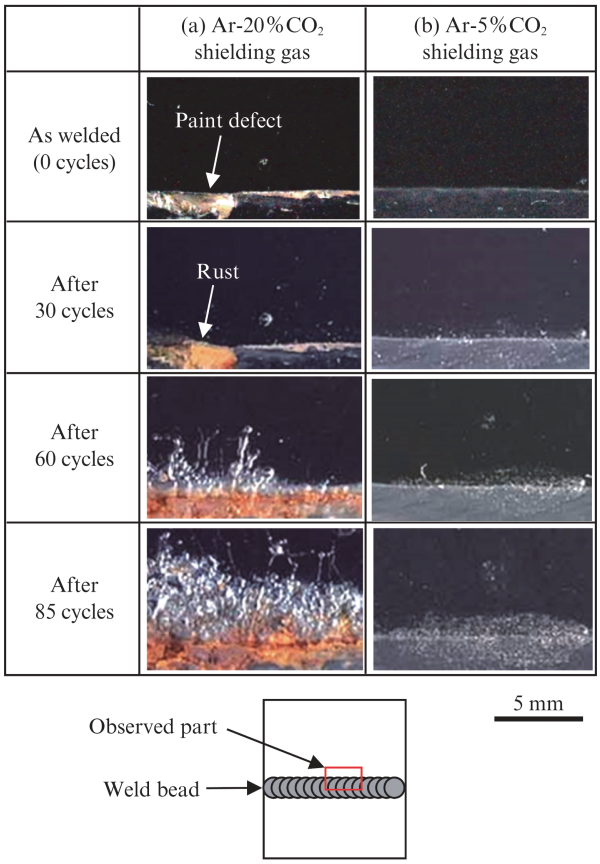

Photo 2 Change in weld part appearance during corrosion test

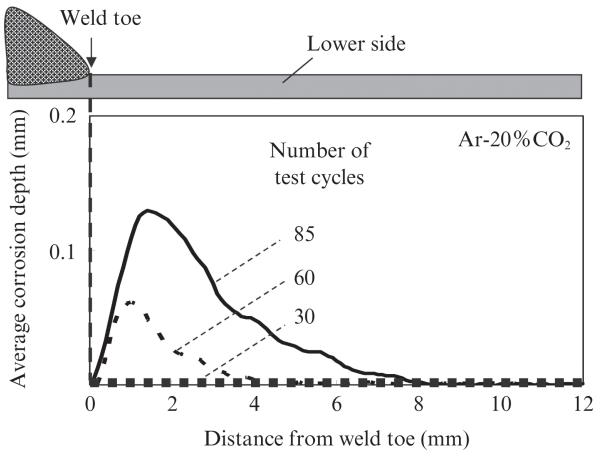

Fig. 2 Change in average corrosion depth near weld toe

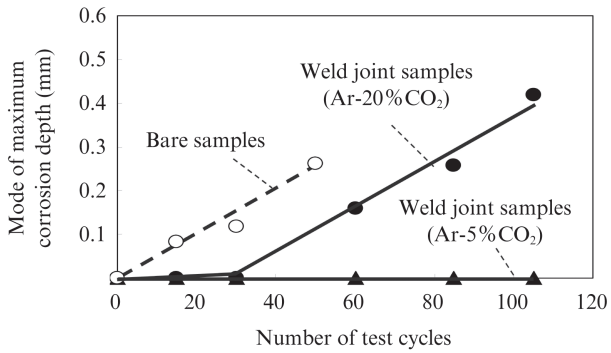

Fig. 3 Change in maximum corrosion depth during corrosion test

welded joints shown in Photo 1 after chemical conversion and electrodeposition coating with a film thickness of 20 μm were performed on the welded joints shown in Photo 1 as general coatings of automotive bodies and chassis. **Photo 2** shows the appearance of the surfaces of the welds in the corrosion test. With the Ar-20% CO_2 shielding gas, paint film defects exist on the weld bead and at the weld toe, and rust initiates from those defects and corrosion proceeds under the paint film. From the results of cross-sectional observation, it was found that these paint film defects originated from slag deposited during welding. On the other hand, with the Ar-5% CO_2 shielding gas, paint film defects were not observed around the bead, and the progress of corrosion was extremely slight.

Figure 2 shows the change in the average corrosion depth near the weld toe with the Ar-20% CO_2 shielding gas. As shown in this figure, the area with the largest corrosion depth is near the weld toe. **Figure 3** shows the change over time in the maximum corrosion depth of the weld in the corrosion test. With the Ar-20% CO_2 shielding gas, the corrosion depth did not increase up to 30 cycles. Although corrosion progressed under the paint film near the weld toe, the corrosion depth of the steel was not on a detectable level and the corrosion protection function of the paint film was considered to be maintained. However, after 30 cycles, corrosion progressed at approximately the same rate (showed the same slope in the graph in Fig. 3) as on the unpainted (bare) samples. This is thought to be due to progress of the corrosion under the paint film that originated from the slag near the weld toe, followed by loss of the corrosion protection function of the paint film due to early film peeling. As a result, corrosion resistance decreased to the level at which the paint film had virtually no corrosion protection effect. On the other hand, with the Ar-5% CO_2 shielding gas, the slag that causes paint film defects did not adhere, and corrosion of the substrate steel was not observed.

Those test results indicate that decreased corrosion resistance of arc welds occurs in the following process: the paint film defects are generated as a result of welding slag adhering near the weld bead and toe, corrosion originating at these paint film defects progresses under the paint film, and then corrosion of the substrate steel proceeds under a condition similar to that of bare material at the parts where the paint film has peeled off. Since the CO_2 gas component is the cause of slag formation, it is thought that corrosion resistance is improved by Ar-5% CO_2 gas shielded arc welding with a reduced CO_2 gas composition because virtually no

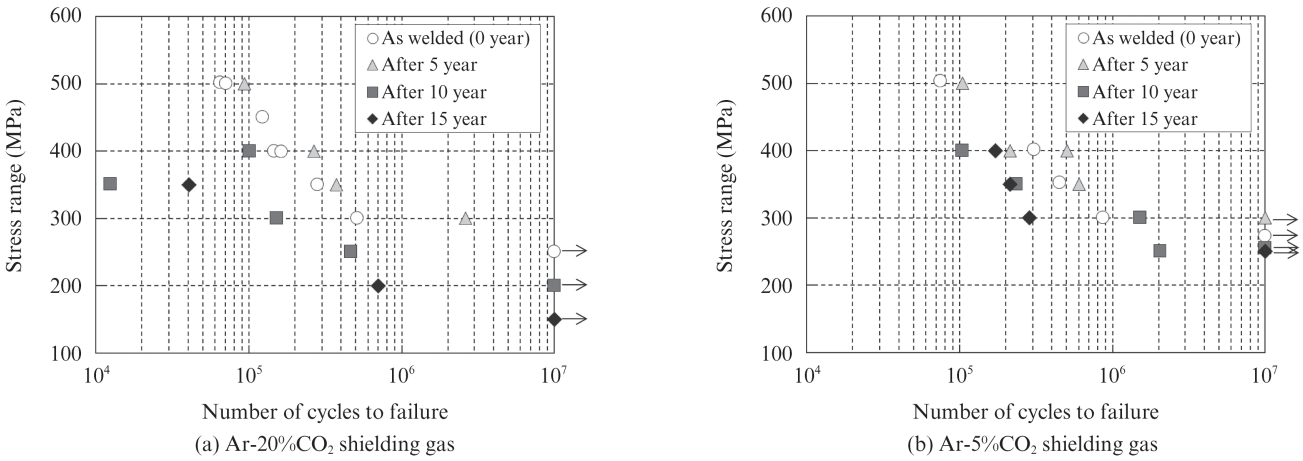

Fig. 4 Change in fatigue strength of welded joints before and after corrosion resistance test

paint film defects occur, and the corrosion protection function of the paint film is maintained even under corrosive environments.

2.4 Influence of Shielding Gas Composition on Fatigue Characteristics of Arc Welded Joints[3)]

Welded joints after corrosion equivalent to the passage of 5 years, 10 years and 15 years in the actual use environment were prepared by a corrosion test, and a complete pulsating fatigue test was conducted using a Schenk-type plane bending fatigue tester. **Figure 4** shows the results of the fatigue test of the welded joints. With welding methods using either the Ar-20% CO_2 or the Ar-5% CO_2 shielding gas, there was almost no change in the fatigue strength of the welded joints before corrosion and after corrosion equivalent to the passage of 5 years, and there was also no difference depending on the shielding gas. In contrast, the fatigue strength after corrosion equivalent to the passage of 10 years and 15 years decreased greatly with the Ar-20% CO_2 shielding gas, but there was virtually no decrease with the Ar-5% CO_2 shielding gas. This difference is due to the fact the formation of welding slag was suppressed by reducing the CO_2 mixing ratio in the shielding gas. Such decrease in slag reduces the corrosion loss around the weld toe, and resultant changes in the joint surface shape and sheet thickness. This result showed that the low CO_2 gas shielded arc welding method has a large effect in suppressing decreased fatigue strength reduction in welded joints after corrosion.

3. Plasma–Arc Hybrid^{TM} Welding Technology

3.1 Problems to be Solved by Plasma–Arc Hybrid^{TM} Welding Technology

As described in the previous chapter, the fatigue strength of welded joints is enhanced by decreasing stress concentration by improving the shape of the weld toe shape, and application of the low CO_2 gas shielded arc welding method is effective for improving the weld toe shape. However, even higher welded joint fatigue strength can also be expected if it is possible to further smoothen the weld toe in comparison with the low CO_2 gas shielded arc welding method. Therefore, as a welding method for obtaining a smoother weld toe, JFE Steel developed the Plasma-Arc Hybrid^{TM} welding technology, which is a hybrid process combining plasma arc welding and CO_2 arc welding[4)].

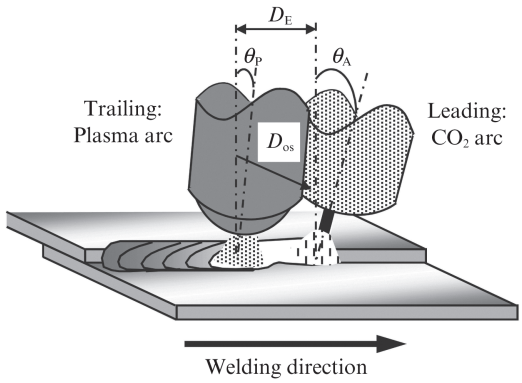

Fig. 5 Electrodes setting of plasma-arc hybrid^{TM} welding

3.2 Bead Shape Improvement Effect by Plasma–Arc Hybrid^{TM} Welding

A comparison of the bead shapes in Plasma-Arc Hybrid^{TM} welding, MAG welding (Ar-20% CO_2 shielding gas) and CO_2 arc welding (100% CO_2 shielding gas) was carried out with lap fillet joints (sheet thickness: 3.2 mm, 780 MPa class hot-rolled steel sheet). **Figure 5** shows a schematic diagram of Plasma-Arc Hybrid^{TM} welding. This is a method in which the trailing plasma arc follows the leading CO_2 arc and combines straight polarity (EN) of the CO_2 arc by using a REM-added

Table 1 Welding conditions of plasma-arc hybrid™ welding and conventional arc welding

Mark	Leading: Arc welding						Trailing: Plasma arc welding						D_E [mm]	Travel speed [mm/min]	Heat Input [kJ/mm]
	Welding wire	θ_A [deg.]	Shielding gas	Polarity	Current [A]	Voltage [V]	θ_P [deg.]	D_{OS} [mm]	Shielding gas	Polarity	Current [A]	Voltage [V]			
PAH	YGW11	30	CO_2	EN	250	27	30	4	Ar	EN	180	23	25	850	0.77
MAG	YGW15	30	Ar-20%CO_2	EP	320	28	–	–	–	–	–	–	–	1 200	0.45
CO_2	YGW11	30	CO_2	EP	220	20	–	–	–	–	–	–	–	600	0.44

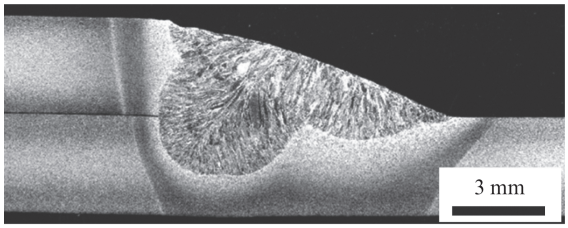

(a) Plasma-arc hybrid™ welding

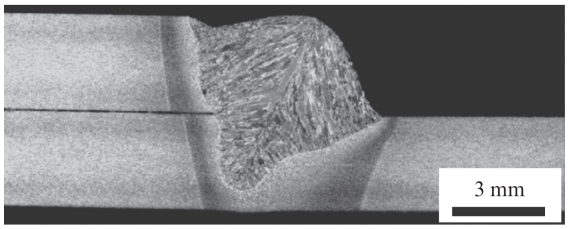

(b) MAG arc welding

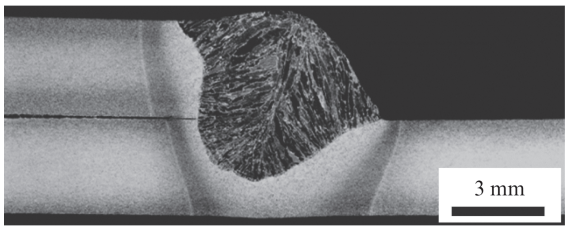

(c) CO_2 arc welding

Photo 3 Macrostructures of cross-sections of welds

Table 2 Weld toe shape for each welding process

	Curvature radius: ρ [mm]	Flank angle: θ [deg.]	Stress concentration factor: K_t
PAH	0.97	161	1.2
MAG	0.46	143	1.5
CO_2	0.41	125	1.7

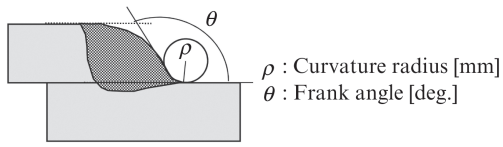

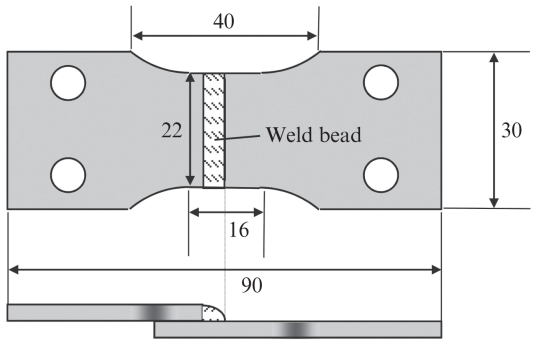

Fig. 6 Fatigue test specimen of welded joint

wire (J-STAR™ welding wire) and also straight polarity (EN) in the plasma arc. As the positional relationship between the CO_2 arc and the plasma arc, the distance between the electrodes (D_E) and the offset (D_{OS}) of the plasma arc welding electrode from the weld centerline of the leading CO_2 arc are properly set, as well as the torch angles. **Table 1** shows the welding conditions of Plasma-Arc Hybrid™ welding, MAG welding and CO_2 arc welding compared here. (The symbols PAH, MAG and CO_2 mean Plasma-Arc Hybrid™ welding, MAG welding and CO_2 arc welding, respectively.) These welding conditions were selected as the optimum conditions at the welding speed considered to be the upper limit when welding lap fillet joints with a sheet thickness of 3.2 mm.

Photo 3 and **Table 2** show the cross-sectional macrostructures of the lap fillet joints in Plasma-Arc Hybrid™ welding, MAG welding and CO_2 arc welding and the results of measurement and calculation of the curvature radius, flank angle and stress concentration factor of the weld toe based on the bead surface shapes in macrostructures. In Plasma-Arc Hybrid™ welding, it can be understood that a bead with a wider surface and a smoother shape in comparison with the other methods can be obtained by superimposition of the penetration of CO_2 arc welding and the plasma arc welding at the proper setting. In the comparison of the stress concentration factor, K_t, calculated from the toe shape, the K_t of Plasma-Arc Hybrid™ welding is reduced to 0.7 to 0.8 times that of MAG welding and CO_2 arc welding. Thus, improvement of joint fatigue strength by smoothening of the weld toe shape can be expected.

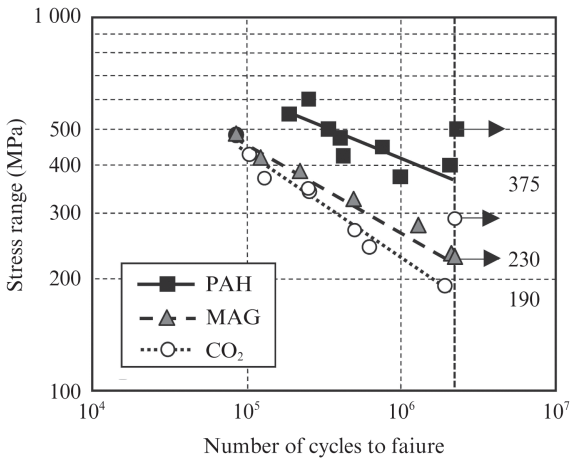

Fig. 7 Fatigue test results of welded joints

3.3 Joint Fatigue Strength Improvement Effect by Plasma–Arc Hybrid™ Welding[4)]

Fatigue test specimens of the welded joints, as shown in **Fig. 6**, were machined from the Plasma-Arc Hybrid™ welding, MAG welding and CO_2 arc welding joints prepared under the welding conditions shown in Table 1, and a complete pulsating fatigue test (upper limit of test cycles: 2×10^6) was conducted using a Schenk-type plane bending fatigue tester. The results are shown in **Fig. 7**. Fatigue strength increased in the order of CO_2 arc welding, MAG welding and Plasma-Arc Hybrid™ welding, and when compared at the fatigue limit (stress range showing endurance at more than 2×10^6 cycles), the Plasma-Arc Hybrid™ welded joint shows a stress range of 375 MPa, or approximately double the 190 MPa of CO_2 arc welded joint. These results confirmed the possibility of a dramatic improvement in joint fatigue strength by smoothening the weld bead shape by applying Plasma-Arc Hybrid™ welding.

4. Laser–Arc Hybrid Welding Technology

4.1 Merits of Laser–Arc Hybrid Welding

In addition to parts with lap welded structures of flat sheets, parts with steel pipe shapes having circular or polygonal cross-sectional shapes called closed cross-section structures are also used in chassis parts. In the future, the adoption of closed cross-section structures of high tensile strength steel is considered to be effective for the need to satisfy both stricter weight reduction requirements and higher mechanical properties, such as rigidity and fatigue strength in the automotive chassis[5)]. In manufacturing parts with closed cross-section structures from flat sheets, welding with the seam part in a butted or lapped joint condition is necessary, but high speed, high efficiency welding by gas shielded arc welding is not possible due to the difficulty of obtaining the necessary welding penetration. On the other hand, in laser welding, the difficulty of controlling the accuracy of the butted or lapped gap to prevent burn through is an issue. Therefore, JFE Steel focused on laser-arc hybrid welding, which has the merits of enabling high speed, high efficiency welding and relaxation of gap accuracy.

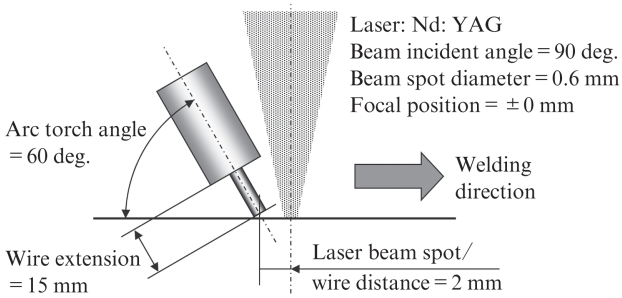

Fig. 8 Settings of laser-arc hybrid welding

Table 3 Welding conditions of laser-arc hybrid welding

Laser power (kW)	3.5 (sheet gap≦0.6 mm) 4.0 (sheet gap≧0.8 mm)
Arc current (A)	80, 160, 240
Welding speed (m/min)	2.5
Shielding gas	Ar-20%CO_2
Welding wire	JIS Z 3312 YGW12 (dia.=0.9 mm)

4.2 Weldability and Joint Characteristics of Laser–Arc Hybrid Welding of Lap Weld Joints[6)]

Laser-arc hybrid welding of lap weld joints (sheet thickness: 1.4 mm, 590 MPa grade galvannealed steel sheets) was performed with the lap face gap (sheet gap) varied in the range from 0 mm to 1.0 mm. In laser-arc hybrid welding, a leading laser beam (Nd: YAG laser) and following MAG arc configuration was used, as shown in **Fig. 8**. The welding conditions were as shown in **Table 3**, and welding was performed while adjusting the laser output and arc current in response to changes in the sheet gap. The strength of the welded joints was evaluated by using tensile shear test specimens with a width of 30 mm shown in **Fig. 9**.

The cross-sectional macrostructures of the welds under typical welding conditions are shown in **Photo 4**, and the relationship between the sheet gap and tensile shear strength under the respective welding conditions is shown in **Fig. 10**. In welding using only a laser beam, pits and burn through occurred with a gap on the order of 0.2 mm. However, with laser-arc hybrid welding, defect-free welding was possible with a sheet gap as large as 0.8 mm, which is equivalent to 50% of the

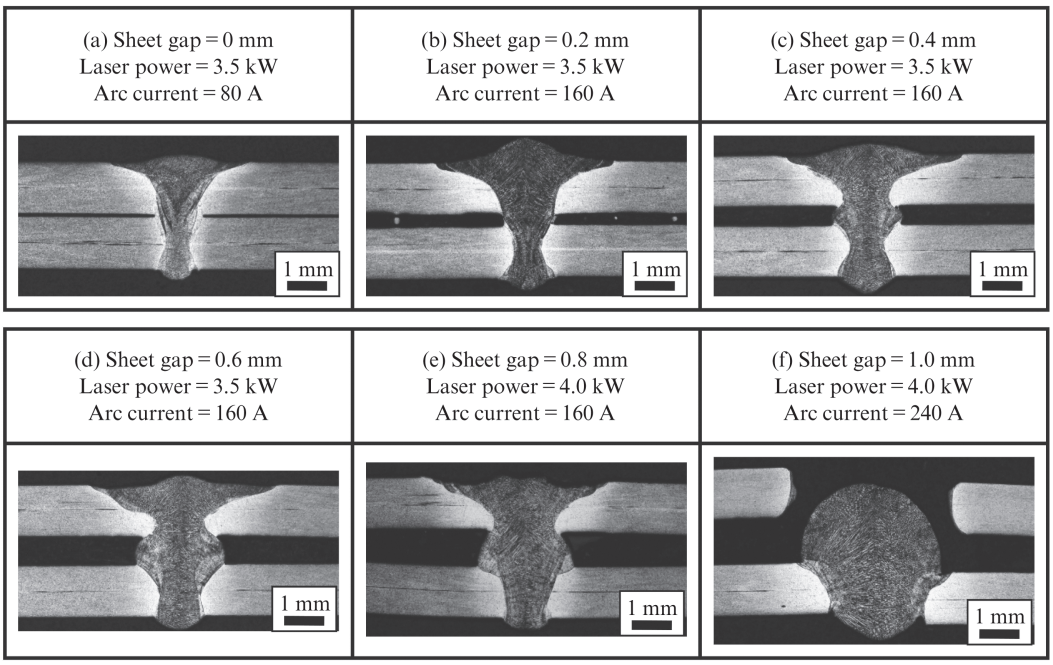

Photo 4 Cross-sectional macrostructures of laser-arc hybrid welds in typical welding conditions

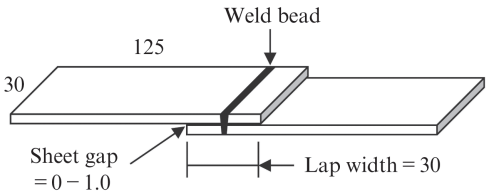

Fig. 9 Dimension of tensile shear test specimen

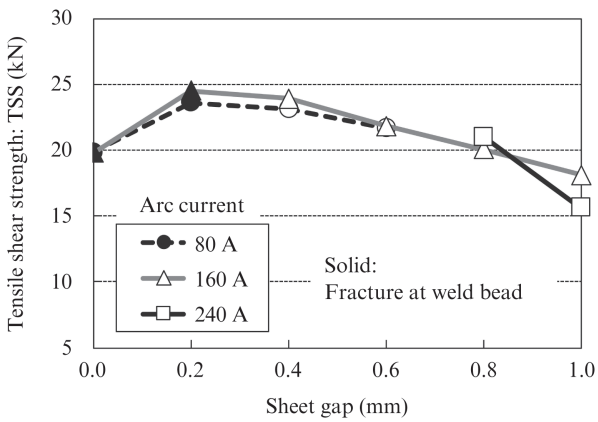

Fig. 10 Tensile shear test results of laser-arc hybrid welded lap joints

sheet thickness. Because underfill and burn through occurred with sheet gaps of 0.6 mm and larger in welding with an arc current of 80A, it was necessary to make adjustments so as to increase the arc current to increase the deposit metal corresponding to increases in the sheet gap. In the investigation of the tensile shear strength of the joints, with the sheet gap of 0 mm, fracture occurred at the weld bead due to blowholes caused by vaporization of the zinc coating, and the tensile shear strength of the joint with the sheet gap of 0 mm was lower than those of the joints with the gaps of 0.2 mm to 0.8 mm. With the sheet gap of 0.2 mm, fracture occurred in the weld metal, and with the gaps of 0.4 mm and larger, fracture occurred in the heat affected zone (HAZ) near the weld metal or in the base material. However, at sheet gaps of 0.2 mm and larger, the tensile strength of the joints tended to decrease as the gap increased. Although this strength decrease is considered to be due to underfill of the bead surface, the extent of the decrease was small, and it was possible to secure a certain joint strength or more even with a large sheet gap.

As described above, laser-arc hybrid welding makes it possible to relax the sheet gap accuracy of lap weld joints in high speed, high efficiency welding, suggesting that this welding method is suitable for production of chassis parts with closed cross-section structures.

5. Conclusion

As welding technologies which enable the improved fatigue characteristics and corrosion resistance demanded in welded joints of automotive chassis parts, as well as high efficiency in the production process, low CO_2 gas shielded arc welding, Plasma-Arc Hybrid™ welding and laser-arc hybrid welding were studied, and welding technologies that realize the following effects were developed.

(1) Use of the low CO_2 gas shielded arc welding

method, in which the mixing ratio of the active gas (CO_2) is reduced, makes it possible to flatten the weld toe and reduce slag generation, resulting in a large improvement in corrosion resistance and fatigue characteristics in the actual use environment.

(2) The Plasma-Arc Hybrid™ welding method enables flattening of the weld toe shape of lap fillet weld joints, thereby realizing a dramatic improvement in the fatigue strength of the joints.

(3) The laser-arc hybrid welding method enables higher speed, higher efficiency welding in comparison with arc welding, and also has the merit of relaxing gap accuracy control of welded joints, suggesting that this is a promising welding technology for application to welding of parts with closed cross-section structures.

References

1) Kataoka, T.; Ikeda, R.; Ueda, S.; Nakazawa, T. Preprints of the National Meeting of J.W.S. 2014, no. 95, p. 50–51.
2) Yamomoto, S.; Suzuki, S.; Ando, S.; Ikeda, R.; Kataoka, T.; Ueda, S.; Nakazawa, T. Preprints of the National Meeting of J. W.S. 2015, no. 97, p. 304–305.
3) Ikeda, R.; Yamomoto, S.; Ando, S.; Kataoka, T.; Ueda, S.; Nakazawa, T. Preprints of the National Meeting of J.W.S. 2015, no. 97, p. 306–307.
4) Matsushita, M.; Kataoka, T.; Ikeda, R.; Endo, S. Quarterly Journal of the J.W.S. 2012, vol. 30, no. 1, p. 77–85.
5) Higai, K.; Shinmiya, T.; Yamasaki, Y. JFE Technical Report. 2013, no. 18, p.103–110.
6) Kitani, Y.; Ikeda, R.; Oi, K. Preprints of the National Meeting of J.W.S. 2013, no. 93, p. 10–11.

Copyright © 2019 JFE Steel Corporation. All Rights Reserved. Unauthorized reproduction prohibited.